ARTICLE

OBC
www.rsc.org/obc

Boron dipyrromethene fluorophore based fluorescence sensor for the selective imaging of Zn(II) in living cells

Yunkou Wu, Xiaojun Peng,* Binchen Guo, Jiangli Fan, Zhichao Zhang, Jingyun Wang, Aijun Cui and Yunling Gao

State Key Laboratory of Fine Chemicals, Dalian University of Technology, 158 Zhongshan Road, Dalian 116012, China. E-mail: pengxj@dlut.edu.cn; Fax: +86-411-88993885; Tel: +86-411-88993899

Received 3rd February 2005, Accepted 3rd March 2005
First published as an Advance Article on the web 16th March 2005

A simple PET fluorescence sensor (BDA) for Zn^{2+} that utilizes 1,3,5,7-tetramethyl-boron dipyrromethene as a reporting group and di(2-picolyl)amine as a chelator for Zn^{2+} has been synthesized and characterized. BDA has an excitation (491 nm) and emission wavelength (509 nm) in the visible range. The fluorescence quantum yields of the zinc-free and zinc-bound states of BDA are 0.077 and 0.857, respectively. With a low pK_a of 2.1 ± 0.1, BDA has the advantage of less sensitivity to pH than fluorescein-based Zn^{2+} sensors, and the fluorescence emission of zinc-binding is pH-independent in the range of pH 3–10. Under physiological conditions, metal ions such as Na^+, K^+, Ca^{2+}, Mg^{2+}, Mn^{2+} and Fe^{2+} have little interference. The apparent dissociation constant (K_d) is 1.0 ± 0.1 nM. Using fluorescence microscopy, the sensor is shown to be capable of imaging intracellular Zn^{2+} changes.

Introduction

Zinc is the second most abundant transition metal ion found in the body, and plays an essential role in many cellular processes,[1] including gene expression,[2] apoptosis,[3] enzyme regulation,[4] and neurotransmission.[5] Recently, there has been a great trend to develop fluorescence sensors suitable for measuring Zn^{2+} in living cells.[6,7,8] Quinoline derivatives (such as TSQ,[9] zinquin[10] and TFLZn[11]) and fluorescein derivatives[7] (such as zinpyr-1, zinpyr-2, ZnAF-1 and ZnAF-2) are two important types of such sensors. However, the quinoline-type sensors are excited at UV wavelengths (~350 nm), which may cause cell damage. The fluorescein-type sensors are pH-sensitive around neutral conditions (pK_a values of 8.4 for zinpyr-1 and 9.4 for zinpyr-2), though chloro or fluoro-substituted fluorescein sensors overcome this problem to a large extent.[7] The pH sensitivity of fluorescein-type sensors contributes to the pH dependence of the excitation and emission spectra of the fluorescein reporting group, in which exist two consecutive transitions with pH change: neutral form–monoanion and monoanion–dianion.[12] Cellular pH change induced by biological stimulation[13] can cause difficulty in interpreting fluorescence intensity change. So there is still scope for improvement in the design of new fluorophores in these sensors.

We describe here a new PET (photoinduced electron transfer)[12,14] fluorescence sensor for Zn^{2+} based on a boron dipyrromethene (BODIPY) platform. BODIPY dyes are relatively insensitive to solvent polarity and pH, more photostable than fluorescein in many environments, and have derivatives that span the visible spectrum with high extinction coefficients, high fluorescence quantum yields (often approaching 1.0, even in water) and narrow emission bandwidths.[15] Currently, a few BODIPY-type fluorescence sensors or switches have been reported.[16] BODIPY-based switches for Zn^{2+} exist, but they work on fluorescent quenching *via* a photoinduced oxidative intramolecular electron transfer mechanism.[12,17] Only one example of a BODIPY-based Zn^{2+} sensor with fluorescence enhancement has been reported recently,[18] but the pH-sensitivity and biological application of that sensor have not been disclosed in detail. As for the chelator for Zn^{2+}, we also chose di(2-picolyl)amine (DPA) which is widely used for the design of new Zn^{2+} sensors.[19] BDA, a water-soluble, turn-on BODIPY–DPA based Zn^{2+} sensor described here, is pH-insensitive in almost the whole pH range (pH 3–11) in the presence of Zn^{2+}.

Results and discussion

Synthesis of BDA

BDA was synthesized according to a method similar to one published previously for the synthesis of BODIPY derivatives,[20] which is shown in Scheme 1. First, compound **2** was synthesized in a one-pot reaction: 2,4-dimethylpyrrole was added to an absolute dichloromethane solution of chloroacetyl chloride under an Ar atmosphere, and the solution was stirred at room temperature for 5 hours, then a solution of triethylamine was added, followed by $BF_3{\cdot}OEt_2$, and stirring was continued for 4 hours; the desired compound was obtained in 35% yield by column purification. Finally, compound **2** and di(2-picolyl)amine (DPA) were mixed together in THF and refluxed for 8 hours. Column separation gave BDA in 45% yield.

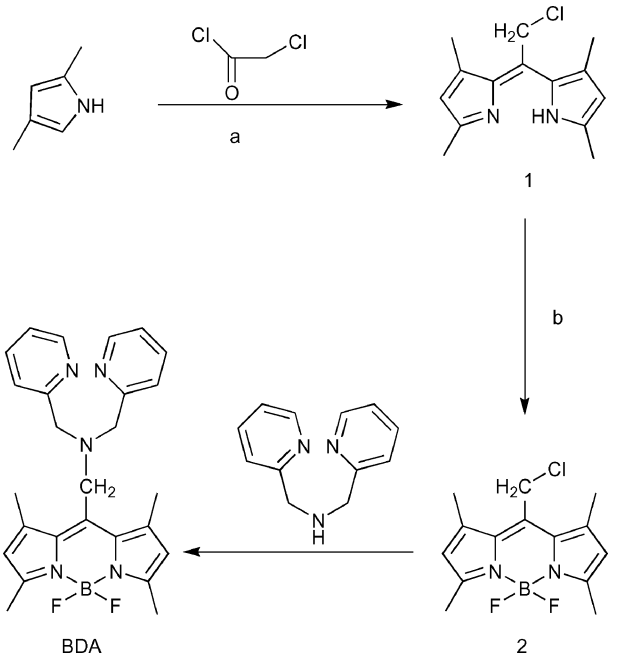

Scheme 1 Synthesis of sensor BDA. Reagents and conditions: (a) CH_2Cl_2, rt, 5 h; (b) CH_2Cl_2, $BF_3{\cdot}OEt_2$, NEt_3, rt, 4 h, 35%; (c) THF, reflux, 8 h, 45%.

DOI: 10.1039/b501795e

^{1}H NMR spectra and molecular models

The ^{1}H NMR spectrum of the boradiazaindacence moiety in BDA shows a great change from that of intermediate **2** (Figs. 1a and 1b). The singlet peak at 2.53 ppm of the four CH_3 groups in **2** splits into four peaks in BDA; the 4.78 ppm peak of the CH_2 spacer in **2** shifts upfield to 4.34 ppm which overlaps with the CH_2 attached to the pyridine rings in BDA; the singlet peak at 6.08 ppm of the protons on the pyrrole rings in **2** splits into two peaks: 6.12 and 6.27 ppm in BDA. The distinguishing spectrum differences between the same parts of two structures imply that the introduction of the DPA moiety leads to great asymmetry strain to the boradiazaindacence moiety in BDA so that the boradiazaindacence moiety is no longer symmetric. To verify the presumption observed by NMR spectroscopy, the conformational properties of the free BDA and **2** were studied by semiempirical calculations. The ground state geometries of them were optimized roughly using a MM2 force field to generate the corresponding coordinates, and further run MOPAC in Chem3D Ultra 7.0 using the AM1 (The Austin Model 1) Hamiltonians.[21] The optimized geometries are shown in Fig. 2. The side-view geometry of **2** illustrates a symmetric planar conformation of the boradiazaindacence moiety, while that of BDA illustrates an asymmetric non-planar conformation, which results from the significant steric repulsion brought about by the presence of the DPA moiety. Relevant geometrical parameters are compiled in Table 1. These data indicate that **2** has an σ-symmetric structure. As for BDA, the distal and proximal methyl groups not only have different bond lengths but also different dihedral angles, and two protons of the pyrrole moieties take exo and endo positions with respect to the C_{19}–C_6 bond, so the protons of the boradiazaindacence moiety in BDA are no longer equivalent.

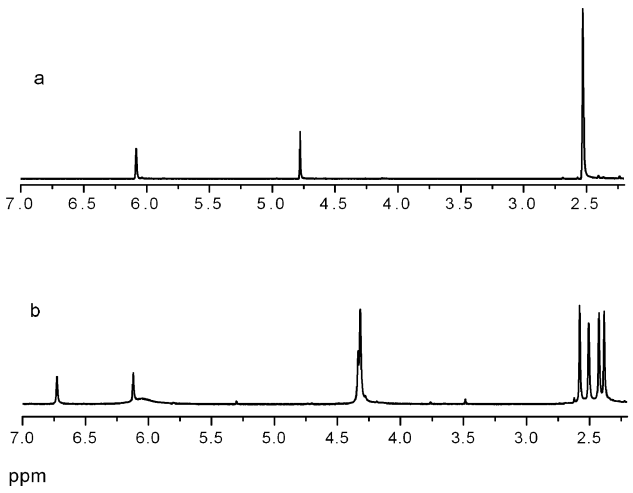

Fig. 1 (a) The partial ^{1}H NMR spectrum of intermediate **2** in $CDCl_3$; (b) the partial ^{1}H NMR spectrum of BDA in $CDCl_3$.

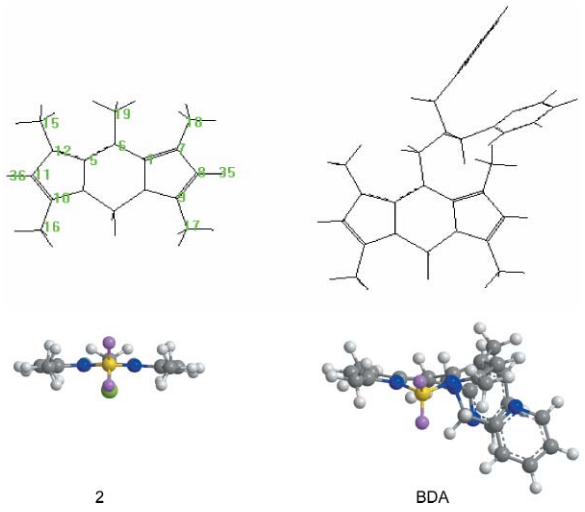

Fig. 2 Simulated structures of **2** and BDA. The top and bottom figures are the side-view and bottom-view of the geometries of **2** and BDA, respectively. The side-view illustrates the planeness of **2** and the curvature of BDA.

Table 1 Selected calculated structural data for **2** and BDA

Parameters[a]	**2**	BDA
r(C_{18}–C_7, nm)	0.1463	0.1464
r(C_{17}–C_9, nm)	0.1463	0.1475
r(C_{16}–C_{10}, nm)	0.1475	0.1476
r(C_{15}–C_{12}, nm)	0.1475	0.1463
r(C_{19}–C_6, nm)	0.1463	0.1487
r(H–C_8, nm)	0.1084	0.1084
r(H–C_{11}, nm)	0.1084	0.1084
f(H–C_8, H–C_{11})	0	5.2
f(C_{18}–C_7, C_{15}–C_{12})	0	15.8
f(C_{17}–C_9, C_{16}–C_{10})	0	7.9
f(C_{18}–C_7, C_{19}–C_6)	7.5	−9.1
f(H_{35}–C_8, C_9–C_{16})	5.1	−17.0
f(H_{36}–C_{11}, C_9–C_{16})	−5.1	19.6

[a] Atom numbering scheme shown in Fig. 2.

Absorption and emission spectra

The absorption and emission properties were investigated in buffered solution (pH 7.4). In the presence of EDTA to scavenge adventitious metal ions, BDA exhibits an absorption maximum wavelength at 491 nm, an emission maximum at 509 nm and a quantum yield of 0.077. The low quantum yield of the bound-free sensor results from photoinduced electron transfer (PET) quenching of the excited state of the boradiazaindacence moiety (electron acceptor) by the lone pair of electrons on the nitrogen atoms (electron donor) in the DPA moiety, which is a photoinduced reductive intramolecular electron transfer process.[12] This is different from that of other BODIPY-based Zn^{2+} switches, which work on fluorescent quenching *via* a photoinduced oxidative intramolecular electron transfer mechanism.[17] Adding Zn^{2+} to the BDA solution, the quenching is disrupted by the coordination of Zn^{2+} with the DPA moiety and the BDA solution shows an intense green fluorescence. The emission maximum of the BDA complex exhibits red shift slightly to 511 nm and the quantum yield increases to 0.857 (~11-fold). Fig. 3 shows the changes in the UV–Vis spectra of BDA at a concentration of 1.0×10^{-5} M upon the addition of Zn^{2+}. A small decrease in the absorption spectra of BDA can be observed by titrating with more than 1 equivalent of Zn^{2+} per ligand into buffered solutions.

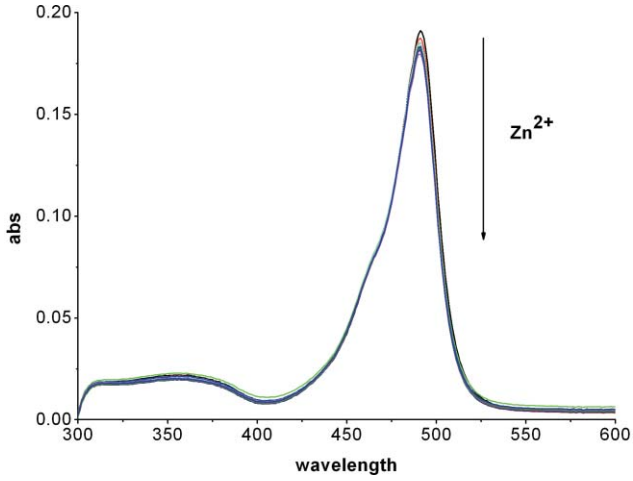

Fig. 3 Absorption spectra of BDA in buffered solution by titration with Zn^{2+}. The concentrations of Zn^{2+} are 0, 0.1, 0.2, 0.3, 0.5, 0.6, 0.7, 0.9, 1.1, 2.0, 3.5 and 5.0 equiv (1 equiv = 1.0×10^{-5}M).

The maximum absorption wavelengths (491 nm) have no shift, and the extinction coefficient changes slightly from 1.95×10^4 to 1.80×10^4 M^{-1} cm^{-1} upon Zn^{2+} binding. The maintaining of the maximum absorption wavelength upon the binding of Zn^{2+} indicates a PET mechanism.[14]

Metal ion selectivity

The fluorescence response of BDA to various cations and its selectivity for Zn^{2+} are examined (Fig. 4). A ~7-fold increase in integrated emission is observed upon addition of Zn^{2+}. Cations such as Na^+, K^+, Ca^{2+} and Mg^{2+}, which exist at high concentrations under physiological conditions, have no influence on fluorescence enhancement. Among the first row transition metal cations, Fe^{2+} and Mn^{2+} show only slight interference on fluorescent enhancement upon the subsequent addition of Zn^{2+}, which implies that BDA has more coordination tendency and selectivity to Zn^{2+} than Fe^{2+} and Mn^{2+}; Cr^{3+} and Co^{2+} afford fluorescence enhancement upon the subsequent addition of Zn^{2+}, but there is some interference; Cu^{2+} and Ni^{2+} induce a decrease of fluorescence intensity because of electron or energy transfer between the metal cations and the fluorophore, a known fluorescence quenching mechanism.[14,22] Similar to behavior in other Zn^{2+} sensors, Cd^{2+} also induces a large fluorescence enhancement and interferes with the selectivity, but the free cations of Cd^{2+} and other interfering ions such as Cu^{2+}, Ni^{2+} and Cr^{3+} would have little influence *in vivo*, since they are not present to a significant extent in ordinary biological systems.[23]

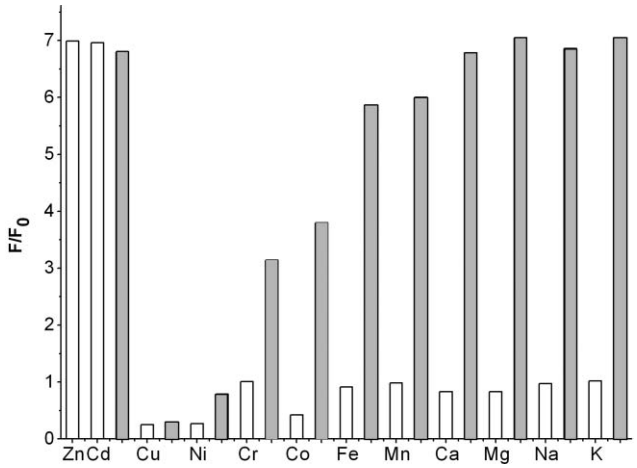

Fig. 4 The fluorescence response of BDA to various cations and its selectivity for Zn^{2+}. The colourless bars represent the integrated emission of BDA in the presence of 20 equiv of the cations of interest; the dark bars represent the changes in integrated emission that occur upon subsequent addition of 20 equiv of Zn^{2+} to solutions containing BDA and the cations of interest. The response was normalized with respect to the integrated emission intensity of free dye (F_0); excitation was provided at 491 nm and emission was integrated from 497 to 600 nm; the slit width was 2 nm for both excitation and emission.

Protonation equilibrium

The common disadvantage of PET-based sensors is the interference of a proton, which also binds with the coordinate site (such as the tertiary nitrogen atom in DPA), inhibits the PET process and enhances the fluorescence. Also, the fluorophores, such as fluorescein, always show pH-sensitivity in fluorescence emission. The fluorescence response of BDA toward pH was investigated in water with an ionic strength of 0.1 (NaCl). Its emission is switched off upon titration with diluted NaOH solution to an acidic solution of BDA (pH ~1.1). The switching is fully reversible. This also demonstrates a typical PET fluorescence on/off effect. The resulting sigmoidal curve (Fig. 5) gives a pK_a of 2.1 ± 0.1, which is much lower than other DPA-based sensors, and BDA is pH-independent in the range of pH 4–

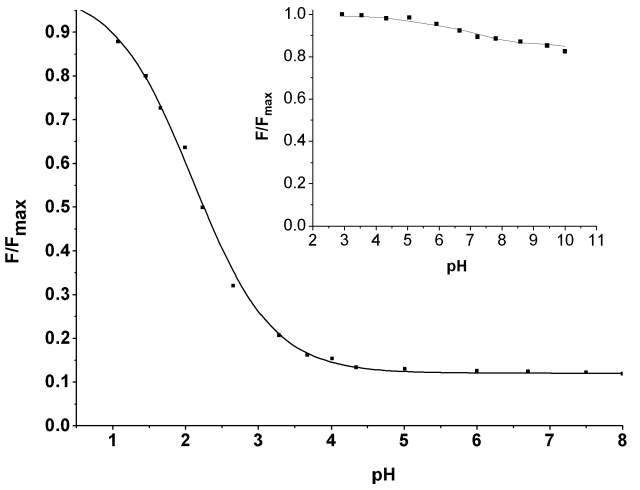

Fig. 5 The normalized integrated emission intensity of BDA *versus* pH. Inset: the normalized integrated emission intensity of the BDA–Zn^{2+} complex *versus* pH. Excitation was at 491 nm and the slit width was 2 nm for both excitation and emission.

10. This may be due to the electron deficiency of the BODIPY fluorophore,[24] which reduces the basicity of the tertiary nitrogen of DPA. Another reason is the stress structure of BDA as described above and the protonation of the tertiary nitrogen atom will lead to greater steric strain. Therefore, the affinity of a proton to the tertiary nitrogen atom becomes more difficult and the pK_a of the BDA is lower than other systems. In the presence of Zn^{2+}, the BDA–Zn^{2+} complex has almost no pH interference from pH 3.0 to 10.0 (inset graph in Fig. 5). This pH-insensitivity is extremely valuable for applications to living cells, where pH changes are caused by certain biological stimuli.

Stoichiometry and the apparent Zn^{2+} dissociation constant

The dissociation constant of BDA complexing with Zn^{2+} was studied in NTA–tris–HCl buffer systems and NaCl maintained ionic strength. The fluorescence titration spectra of BDA with Zn^{2+} are shown in Fig. 6a. A Hill plot was made to obtain the stoichiometry, and it was plotted according to the following equation:

$$\log\left(\frac{F - F_{\min}}{F_{\max} - F}\right) = \log K_s + \log[M]$$

$F_{\min}$ and $F_{\max}$ are the integrated emission intensities in the absence of and with an excess of Zn^{2+}, respectively. K_s is the stability constant. $[M]$ is the free concentration of Zn^{2+}. The fluorescence response fits to a Hill coefficient of 1 (inset graph in Fig. 6b); it is consistent with the formation of a 1 : 1 stoichiometry for the BDA–Zn^{2+} complex. By plotting the normalized integrated emission intensity changes with $p[Zn^{2+}]_{free}$, a sigmoidal curve (Fig. 6b) is obtained and the dissociation constant, K_d, is deduced to be 1.0 ± 0.1 nM, which indicates that BDA can quantitatively measure the concentration of Zn^{2+} around the nanomolar range. This value is similar to other DPA-based Zn^{2+} sensors. As expected, the binding of BDA is fast and is completed upon mixing ligand and metal.

Microscopy images

Biological applications of BDA were evaluated *in vivo*. First, the cultured TCA cells were incubated with 10 μM BDA (from 1mM solution in DMSO) for 5 min, which was sufficient time for the intracellular accumulation of BDA judging from its weak self-fluorescence inside a living cell (Fig. 7a). Prompt increases in the fluorescence intensity in living cells were observed upon the addition of Zn^{2+} (50 μm) into the medium and after co-contribution for 30 min at 37 °C (Fig. 7b). Further investigations were carried out with PC12 cells. BDA-labeled PC12 cells,

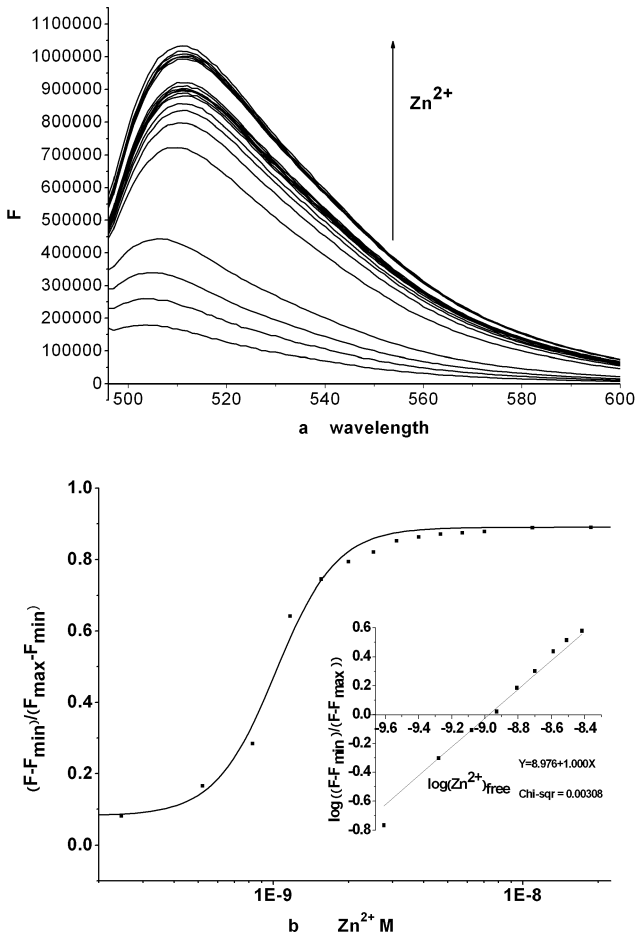

Fig. 6 (a) Fluorescence emission spectra of BDA in buffered Zn^{2+} solutions with free Zn^{2+} concentrations of 0, 0.25, 0.52, 0.83, 1.17, 1.56, 2.00, 2.52, 3.12, 3.83, 4.68, 5.72, 7.02, 10.92 and 18.72 nM; for several of the final spectra, additional $ZnSO_4$ was added to provide the concentrations of free Zn^{2+} from ~5 to ~25 μM. (b) The normalized integrated emission intensity *versus* the $p[Zn^{2+}]_{free}$. Inset: the Hill plot of BDA complexation with Zn^{2+}. The slit width was 2 nm for both excitation and emission.

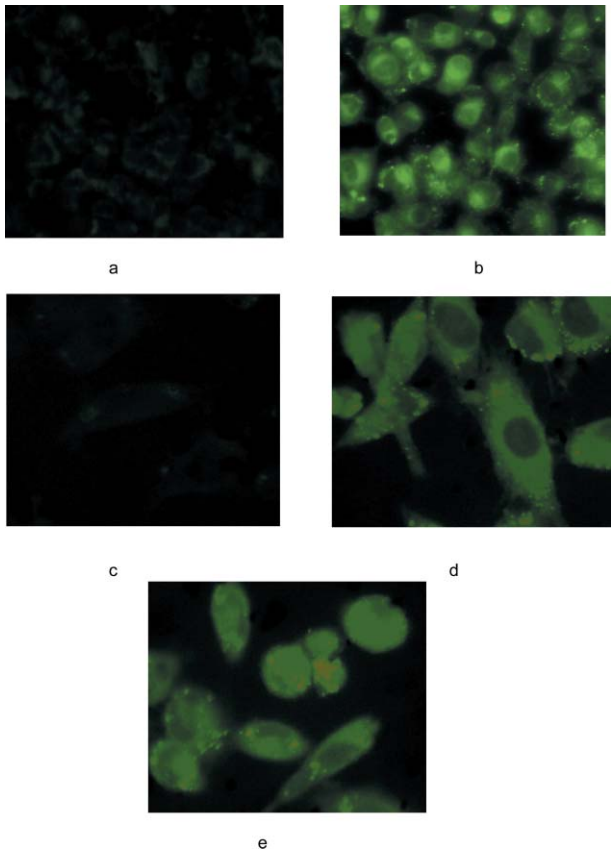

Fig. 7 (a) Fluorescence image of TCA cells loaded with BDA. The cells were incubated with 10 μM BDA for 5 min at 37 °C, under 5% CO_2. Then the cells were washed with phosphate buffered saline (PBS, pH = 7.4) 3 times. (b) Fluorescence image of BDA stained cells loaded with 50 μm Zn^{2+} for 30 min. (c) Fluorescence image of PC12 cells untreated with Zn^{2+} and SNP. (d) Fluorescence image of the PC12 cells loaded with 1 μm Zn^{2+}. (e) Fluorescence image of the PC12 cells treated with SNP. The excited light is WB 450–480 nm.

untreated with $ZnCl_2$ and SNP, showed a weak fluorescence in their cytoplasm with nuclei always unlabeled (Fig. 7c). But the cell preloaded with Zn^{2+} (1 μm) exhibited a strong fluorescence in the cytoplasm as well as in the nuclei (Fig. 7d). The same result was also observed with cells treated with SNP (Fig. 7e). This is because SNP is an NO donor; NO mediates intracellular and intranuclear Zn^{2+} release, resulting in the increase of fluorescence intensity in the cytoplasm and nuclei. This data also indicated that the lack of fluorescence in control nuclei is not due to the inability of BDA to enter the nuclei. All these results suggested that BDA can be used to monitor changes of intracellular Zn^{2+} in a living cell, and should therefore be useful for clarifying the role of Zn^{2+} in biological processes in which the intracellular concentration changes of Zn^{2+} are important, for example, cell death induced by ischemia and AD, PD diseases.[25]

Conclusions

In summary, we have reported a novel and simple fluorescence sensor for Zn^{2+} by utilizing BODIPY as the reporting group. This sensor can work in aqueous solution and has good selectivity and nanomolar sensitivity. It has overcome the primary shortcoming of most fluorescein-type Zn^{2+} sensors and its fluorescence emission is pH-independent under a large physiological pH range. The low toxicity and cell-permeability of this sensor has made it a new Zn^{2+} sensor suitable for biological application. By chemical modification of the BODIPY fluorophore, similar kinds of Zn^{2+} sensors can be designed with absorption and emission maxima spanning the visible spectrum.

Experimental

General notes and procedures

^1H NMR and ^{13}C NMR spectra were obtained on a Varian INVOA 400 MHz spectrometer. Chemical shifts (δ) were reported in ppm relative to a Me_4Si standard in $CDCl_3$. Mass spectra were measured on a HP 1100 LC-MS spectrometer. Elemental analyses were determined using a Perkin-Elmer 204B elemental autoanalyzer. Steady-state emission and excitation spectra were recorded with a PTI-700 fluorimeter and FELIX software. All fluorescence emission spectra have been corrected for the spectral response of the detection system (emission correction file provided by instrument manufacturer). Absorption spectra were determined on a HP8453-Shimadzu UV3100 spectrophotometer. All pH's were measured with a Model PHS-3C meter. Melting points were determined by an X-6 micro-melting point apparatus and are uncorrected. Fluorescent microscope experiments were carried out with a NIKON, TE200 fluorescent microscope.

All solvents and reagents used were reagent grade. All reactions were carried out under an Ar atmosphere with dry, freshly distilled solvents under anhydrous conditions. Tetrahydrofuran was distilled from sodium–benzophenone, and methylene chlorine was distilled from calcium hydride. Di-(2-picolyl)amine (DPA) was prepared as previously described.[26] Silica gel (100–200 mesh) and neutral aluminium oxide (100 mesh) were used for flash column chromatography.

All the fluorescence spectra and absorption spectra were measured in 20 mM tris–HCl buffer solution at pH 7.4, ionic strength was maintained by 100 mM NaCl, except the pH titration. A stock solution of BDA in DMSO (1 mM) was diluted to final concentration prior to use. Metal ions used for the metal selectivity study were Na^+, K^+, Ca^{2+}, Mg^{2+}, Zn^{2+}, Cd^{2+}, Co^{2+}, Cr^{3+}, Cu^{2+}, Mn^{2+}, Ni^{2+} and Fe^{2+}. For Fe^{2+} and Cu^{2+}, stock solutions were prepared in degassed water and diluted to BDA buffer solutions, which were also sparged with N_2 for ten minutes prior to use.

8-(Chloromethyl)-4,4-difluoro-1,3,5,7-tetramethyl-4-bora-3*a*,4*a*-diaza-*s*-indacene (2)

Chloroacetyl chloride (217 mg, 1.94 mmol) and 1,4-dimethylpyrrole (370 mg, 3.9 mmol) were dissolved in 150 ml of absolute CH_2Cl_2 under an Ar atmosphere, the absolute CH_2Cl_2 was sparged with N_2 for 0.5 hour prior to use. Then the mixture was stirred for 5 hours at room temperature. The black solution was reduced to 50 ml, and to the resulting solution was added 4 ml of triethylamine, followed by 8 ml of $BF_3{\cdot}OEt_2$. The mixture was stirred under an Ar atmosphere for another 4 hours at room temperature. Finally, the reaction mixture was washed with water, dried over K_2CO_3, filtered, and evaporated to dryness. The crude compound was purified by flash column chromatography on silica gel (16 : 1 hexanes–EtOAc) to afford a red solid (169 mg, 35%). (Found: C, 56.81; H, 5.51; N, 9.50. Calcd for $BC_{14}ClF_2H_{16}N_2$: C, 56.70; H, 5.44; N, 9.45%.); δ_H(400 MHz; $CDCl_3$; Me_4Si) 2.53 (12H, s, CH_3), 4.78 (2H, s, $ClCH_2C$), 6.08 (2H, s, CH); δ_C(400 MHz; $CDCl_3$; Me_4Si) 14.86, 15.69, 37.33, 122.46, 131.57, 136.14, 141.31, 156.83; δ_F(400 MHz; $CDCl_3$; $CFCl_3$) −146.73 (q, $J = 36$ Hz); mp: 176–178 °C; *m*/*z* (ES) 319 ([M + Na^+], 10%), 297 ([M + H^+], 38), 279 (100).

8-{[Bis(pyridin-2-ylmethyl)amino]methyl}-4,4-difluoro-1,3,5,7-tetramethyl-4-bora-3*a*,4*a*-diaza-*s*-indacene (BDA)

A suspension of **2** (100 mg, 0.34 mmol), di(2-picolyl)amine (67 mg, 0.34 mmol), potassium iodide (60 mg, 0.36 mmol) and potassium carbonate (55 mg, 0.34 mmol) in 50 ml THF was refluxed for 8 hours under an Ar atmosphere. The mixture was cooled to room temperature. THF was removed by evaporation, and the residue was diluted with 20 ml 2 N sodium carbonate and extracted with dichloromethane. The organic phase was washed with brine, dried over K_2CO_3, filtered, and evaporated to dryness. The crude compound was purified by flash column chromatography on neutral aluminium oxide (100 : 1 CH_2Cl_2–MeOH) to afford a yellow solid (62 mg, 45%). (Found: C, 68.12; H, 6.22; N, 15.34. Calcd for $BC_{26}F_2H_{28}N_5$: C, 67.98; H, 6.14; N, 15.25%.); δ_H(400 MHz; $CDCl_3$; Me_4Si) 2.38 (3H, s, CH_3), 2.43 (3H, s, CH_3), 2.51 (3H, s, CH_3), 2.58 (3H, s, CH_3), 4.32 (4H, s, $PhCH_2N$), 4.34 (2H, s, CCH_2N), 6.12 (1H, s, CH), 6.72 (1H, s, CH), 7.30 (2H, t, *J* 6.0, ArH), 7.74–7.81 (4H, m, ArH), 8.65 (2H, d, *J* 4.4, ArH); δ_C(400 MHz; $CDCl_3$; Me_4Si) 14.67, 16.63, 17.55, 17.74, 29.88, 30.52, 51.98, 60.95, 119.86, 122.09, 122.76, 132.57, 133.32, 138.85, 140.55, 142.01, 152.33, 154.95, 155.24, 159.69; δ_F(400 MHz; $CDCl_3$; $CFCl_3$) −144.92 (q, $J = 36$ Hz); mp: 62–63 °C; *m*/*z* (ES) 460 ([M + H^+]).

Determination of quantum yields

The quantum yields of BDA were determined at 20 °C according to the literature.[7] Fluorescein ($\phi = 0.90$) in 0.1 N NaOH was used as a standard.[27] For the metal-free study, a 10 ml solution of 1 μM BDA was prepared, and 10 μL of 100 mM Na_4EDTA were added to chelate any adventitious metal ions. The absorption of standard was adjusted to the same value (abs <0.1, 491 nm) as that of BDA. Excitation was chosen at 491 nm; the emission spectra were corrected and integrated from 497 to 650 nm. For the metal-bound studies, 20 μL of a 10 mM $ZnSO_4$ solution were added to a 10 ml solution of 1 μM BDA. In the same way, the absorption was adjusted and the emission spectra were corrected and integrated from 497 to 650 nm. The quantum yields were calculated with the following expression:

$$\Phi_{sample} = \Phi_{standard} \times \frac{\int \text{emission}_{sample}}{\int \text{emission}_{standard}}$$

Determination of protonation constant

The pK_a of BDA was measured in a 100 mM NaCl water solution. In a typical experiment, a 20 ml solution of 1 μM BDA containing 100 mM NaCl and ~100 mM HCl was prepared. Diluted NaOH solution was added to achieve the appropriate pH change from 1.1 to 11.5. The overall volume change did not exceed 2%. Excitation was provided at 491 nm and emission was integrated from 497 to 600 nm. The response was normalized with respect to maximum integrated emission intensity and the data were fitted to a sigmoidal curve.

Determination of dissociation constant

The dissociation constant of BDA was determined according to the literature.[7,28] In a typical experiment, 5 μL of a 1 M $ZnSO_4$ solution were added to 10 ml buffer solutions (20 mM tris–HCl, pH 7.4) containing 100 mM NaCl and 10 mM nitrilotriacetic acid (NTA). For each addition, the integrated emission intensity change was recorded. The overall concentration of $ZnSO_4$ changed from 0 to 9 mM, and the free Zn^{2+} changed from 0, 0.246, 0.52, 0.826, 1.17, 1.56, 2, 2.52, 3.12, 3.83, 4.68, 5.72, 7.02, 10.92 to 18.72 nM. For several of the final additions, $ZnSO_4$ solution was added to provide the concentration of free Zn^{2+} changing from ~5 to ~25 μM. The overall volume change did not exceed 2%. Excitation was provided at 491 nm and emission was integrated from 497 to 600 nm. The response was normalized with respect to maximum integrated emission intensity and these data were fitted to a sigmoidal curve.

Cell culture and labeling of cells

PC12 cells were cultured in DEME (Invitrogen) supplemented with 10% FCS (Invitrogen). One day before imaging, cells were placed in 24-well flat-bottomed plates. The next day, part of the PC12 cells were incubated with 10 μM BDA for 1 hour at 37 °C under 5% CO_2 as a control, part of the cells were incubated with BDA in the presence of 10 mM SNP (sodium nitroprussiate) for 1 hour and the rest of the PC12 cells were incubated with 1 μM $ZnCl_2$ for 1 h at 37 °C and then washed with DEME before incubating with 10 μM BDA.

Acknowledgements

This work was supported by the Ministry of Education of China and the National Science Foundation of China (20128005, 20376010 and 20472012). We thank Erhu Lu for helpful discussions and Hongbing Zhang for instruction about fluorescence measurement.

References

1 B. L. Vallee and K. H. Falchuk, *Physiol. Rev.*, 1993, **73**, 79–118; S. J. Lippard, J. M. Berg, *Principles of Bioinorganic Chemistry*, University Science Books, Mill Valley, 1994; R. M. Roat-Malone, *Bioinorganic Chemistry: A Short Course*, John Wiley & Sons, New Jersey, 2002.
2 K. H. Falchuk, *Mol. Cell. Biochem.*, 1998, **188**, 41–48.
3 P. D. Zalewski, I. J. Forbes and W. H. Betts, *Biochem. J.*, 1993, **296**, 403–408.
4 W. Maret, C. Jacob, B. L. Vallee and E. H. Fischer, *Proc. Natl. Acad. Sci. USA*, 1999, **96**, 1936–1940.
5 M. P. Cuajungco and G. J. Lees, *Neurobiol. Dis.*, 1997, **4**, 137–169; D. W. Choi and J.-Y. Koh, *Annu. Rev. Neurosci.*, 1998, **21**, 347–375.
6 E. Kimura and T. Koike, *Chem. Soc. Rev.*, 1998, **27**, 179–184; S. C. Burdette and S. J. Lippard, *Coord. Chem. Rev.*, 2001, **216–217**, 333–361; P. J. Jiang and Z. J. Guo, *Coord. Chem. Rev.*, 2004, **248**, 205–229;

K. Kikuchi, K. Komatsu and T. Nagano, *Curr. Opin. Chem. Biol.*, 2004, **8**, 182–191.
7 S. C. Burdette, G. K. Walkup, B. Spingler, R. Y. Tsien and S. J. Lippard, *J. Am. Chem. Soc.*, 2001, **123**, 7831–7841; S. C. Burdette, C. J. Frederickson, W. Bu and S. J. Lippard, *J. Am. Chem. Soc.*, 2003, **125**, 1778–1787; T. Hirano, K. Kikuchi, Y. Urano, T. Higuchi and T. Nagano, *J. Am. Chem. Soc.*, 2000, **122**, 12399–12400; T. Hirano, K. Kikuchi, Y. Urano and T. Nagano, *J. Am. Chem. Soc.*, 2002, **124**, 6555–6562.
8 K. R. Gee, Z.-L. Zhou, W.-J. Qian and R. Kennedy, *J. Am. Chem. Soc.*, 2002, **124**, 776–778; T. Gunnlaugsson, T. C. Lee and R. Parkesh, *Org. Biomol. Chem.*, 2003, **1**, 3265–3267; M. Taki, J. L. Wolford and T. V. O'Halloran, *J. Am. Chem. Soc.*, 2004, **126**, 712–713; N. C. Lim and C. Breckner, *Chem. Commun.*, 2004, **126**, 1094–1095; M. M. Henary, Y. G. Wu and C. Fahrni, *Chem. Eur. J.*, 2004, **10**, 3015–3025.
9 C. J. Frederickson, E. J. Kasarskis, D. Ringo and R. E. Frederickson, *J. Neurosci. Methods*, 1987, **20**, 91–103.
10 P. D. Zalewski, I. J. Forbes, R. Borlinghaus, H. W. Betts, S. F. Lincoln and A. D. Ward, *Chem. Biol.*, 1994, **1**, 153–161; P. D. Zalewski, S. H. Millard, I. J. Forbes, O. Kapaniris, A. Slavotinek, W. H. Betts, A. D. Ward, S. F. Lincoln and I. Mahadevan, *J. Histochem. Cytochem.*, 1994, **42**, 877–884.
11 T. Budde, A. Minta, J. A. White and A. R. Kay, *Neuroscience*, 1997, **79**, 347–358.
12 B. Valeur, in *Molecular Fluorescence: Principles and Applications*, Wiley-VCH, Weinheim, 2002.
13 J. Li and A. J. Eastman, *Biol. Chem.*, 1995, **270**, 3203–3211.
14 A. P. de Silva, H. Q. N. Gunaratne, T. Gunnlaugsson, A. J. M. Huxley, C. P. McCoy, J. T. Rademacher and T. E. Rice, *Chem. Rev.*, 1997, **97**, 1515–1566; A. P. de Silva, B. McCaughan, O. F. McKinney and M. Querol, *Dalton Trans.*, 2003, **97**, 1902–1913.
15 J. Karolin, L. B.-A. Johansson, L. Strandberg and T. Ny, *J. Am. Chem. Soc.*, 1994, **116**, 7801–7806; R. P. Haughland, *Handbook of Fluorescent Probes and Research Chemicals*, Molecular Probes, Eugene, 6th edn., 1996.
16 K. Rurack, M. Kollmannsberger, U. Resch-Genger and J. Daub, *J. Am. Chem. Soc.*, 2000, **122**, 968–969; K. R. Gee, A. Rukavishnikov and A. Rothe, *Comb. Chem. High Throughput Screening*, 2003, **6**(4), 363–366; N. R. Cha, S. Y. Moon and S.-K. Chang, *Tetrahedron Lett.*, 2003, **44**(4), 8265–8268; S. Y. Moon, N. R. Cha, Y. H. Kim and S.-K. Chang, *J. Org. Chem.*, 2004, **69**(4), 181–183; Y. Gabe, Y. Urano, K. Kikuchi, H. Kojima and T. Nagano, *J. Am. Chem. Soc.*, 2004, **126**(4), 3357–3367.
17 B. Turfan and E. U. Akkaya, *Org. Lett.*, 2002, **4**, 2857–2859; C. Goze, G. Ulrich, L. Charbonnière, M. Cesario, T. Prangé and R. Ziessel, *Chem. Eur. J.*, 2003, **9**, 3748–3755.
18 H. Koutaka, J. Kosuge, N. Fukasaku, T. Hirano, K. Kikuchi, Y. Urano, H. Kojima and T. Nagano, *Chem. Pharm. Bull.*, 2004, **52**(6), 700–703.
19 S. A. de Silva, A. Zavaleta, D. E. Baron, O. Allam, E. V. Isidor and N. Kashimura, *Tetrahedron Lett.*, 1997, **38**(13), 2237–2240; J. L. Fan, Y. K. Wu and X. J. Peng, *Chem. Lett.*, 2004, **33**(10), 1392–1393.
20 J. Chen, A. Burghart, A. Derecskei-Kovacs and K. Burgess, *J. Org. Chem.*, 2000, **65**, 2900–2906.
21 J. Chen, J. Reibenspies, A. Derecskei-Kovacs and K. Burgess, *Chem. Commun.*, 1999, 2501–2502.
22 L. Fabbrizzi, M. Licchelli, P. Pallavicini, D. Sacchi and A. Taglietti, *Analyst*, 1996, **121**, 1763–1768.
23 T. D. Rae, P. J. Schmidt, R. A. Pufahl, V. C. Culotta and T. V. O'Halloran, *Science*, 1999, **284**, 805–808.
24 M. Kollmannsberger, T. Gareis, S. Heinl, J. Breu and J. Daub, *Angew. Chem., Int. Ed. Engl.*, 1997, **36**, 1333–1335.
25 J.-M. Lee, G. J. Zipfel, K. H. Park, Y. Y. He, C. Y. Hsu and D. W. Choi, *Neuroscience*, 2002, **115**(3), 871–878; M. P. Cuajungco and G. Lees, *Neurobiol. Dis.*, 1997, **4**(3), 137–169.
26 D. W. Gruenwedel, *Inorg. Chem.*, 1968, **7**, 495–501.
27 J. N. Demas and G. A. Crosby, *J. Phys. Chem.*, 1971, **75**, 991–1024.
28 K. A. Connors, in *Binding Constants: The Measurement of Molecular Complex Stability*, John Wiley & Sons, New York, 1987.